Global Allocation Rules for Patterns of Biomass Partitioning in Seed Plants

Article *in* Science · March 2002

DOI: 10.1126/science.1066360 · Source: PubMed

2 authors:

Brian J. Enquist
The University of Arizona
447 PUBLICATIONS **35,425** CITATIONS
SEE PROFILE

Karl J Niklas
Cornell University
481 PUBLICATIONS **20,936** CITATIONS
SEE PROFILE

Global Allocation Rules for Patterns of Biomass Partitioning in Seed Plants

Brian J. Enquist[1,2]* and Karl J. Niklas[3]

A general allometric model has been derived to predict intraspecific and interspecific scaling relationships among seed plant leaf, stem, and root biomass. Analysis of a large compendium of standing organ biomass sampled across a broad sampling of taxa inhabiting diverse ecological habitats supports the relations predicted by the model and defines the boundary conditions for above- and below-ground biomass partitioning. These canonical biomass relations are insensitive to phyletic affiliation (conifers versus angiosperms) and variation in averaged local environmental conditions. The model thus identifies and defines the limits that have guided the diversification of seed plant biomass allocation strategies.

Despite its importance to ecology, global climate research, and evolutionary and ecological theory, the general principles underlying how plant metabolic production is allocated to above- and below-ground biomass remain unclear (*1*–*6*). Indeed, there are few large data sets with which to evaluate patterns of standing biomass within and across the broad spectrum of vascular plant species (*2*, *7*). The resulting uncertainty severely limits the accuracy of models for many ecologically and evolutionarily important phenomena across taxonomically diverse communities (*8*–*11*). Thus, although quantitative assessments of biomass allocation patterns are central to biology, theoretical or empirical assessments of these patterns remain contentious (*2*, *8*, *10*, *11*).

Nonetheless, the scaling relations among standing leaf, stem, and root (below-ground) biomass (M_L, M_S, and M_R, respectively) can be derived analytically by first noting that the amount of resource used per individual plant, $\dot{R}_0$, approximates metabolic demand and gross photosynthesis (B) (*12*–*14*). Because B is predicted to scale proportionally to total M_L ($\dot{R}_0 \propto B \propto M_L$), theory predicts that the surface areas over which resources are exchanged with the environment (e.g., leaf surface area, which correlates with M_L) are proportional to the 3/4 power of the total plant biomass (M_T) (*12*–*14*). Thus, $B \propto M_L \propto M_T^{3/4}$ and $M_L \propto D_S^2$, where D_S is stem diameter. Empirical studies confirm that plant metabolic rate scales as the 3/4 power of M_T (which equals the sum of M_L, M_S, and M_R) and that metabolic rates scale isometrically with respect to M_L (*7*, *12*, *13*, *15*). Here, we extend this theory (*16*) on the basis of three assumptions: (i) Stem and root bulk tissue densities are approximately constant during ontogeny (*13*), (ii) the effective hydraulic cross-sectional areas of stems and roots are equivalent (owing to the conservation of water mass flowing through a plant) (*17*, *18*), and (iii) stem length scales roughly isometrically with respect to root length (L_R). If valid, these three basic assumptions corroborate the predictions that standing M_L will scale as the 3/4 power of M_S and as the 3/4 power of M_R and that standing M_S and M_R will scale isometrically with respect to each other ($M_L \propto M_S^{3/4} \propto M_R^{3/4}$ and $M_S \propto M_R$). It also follows that above-ground biomass (M_A) will scale in a nearly isometric manner with respect to M_R (i.e., $M_L + M_S \propto M_R$) across and within clades and different habitats.

These predictions were tested against data gathered from a variety of sources for standing M_L, M_S, and M_R per plant across monocot, dicot, and conifer species differing by ~nine orders of magnitude in total body mass (*19*–*21*) [see supplemental data (*22*)]. Regression analyses (*21*) of these data show that all observed scaling exponents (α_{RMA}) comply remarkably well with those predicted by the model (Table 1). For example, M_L scales across species as the 1.99 power [95% confidence interval (CI) = $1.90 \leq \alpha_{RMA} \leq 2.07$] of D_S (Fig. 1) and does not differ significantly between angiosperm and conifer species (Table 1). Likewise, comparisons between angiosperm and conifer species reveal no statistically significant variation in the scaling exponents for standing M_L, M_S, and M_R, whereas the relation between M_A and M_R is nearly isometric for mature individuals, as predicted (i.e., $M_A = 3.88 M_R^{1.02}$) (Fig. 2). Within the larger size ranges, statistical outliers are remarkably absent from all bivariant plots even when data from arborescent palm species, which lack a branched growth habit, are included (Figs. 1 and 2). However, our theory predicts a nonlinear log-log relation between M_A and M_R for plants less than 1 year old (*16*). This is not evident in our data for juvenile plants (i.e., less than 1 year old), which are best approximated by a linear log-log curve (Fig. 2). We attribute the departure of these data from theoretical expectations to the influence of nutrients provided by endosperm or megagametophyte tissues on the biomass partitioning pattern attending seedling establishment. Such a "maternal resource compartment" is expected to favor M_R as opposed to M_A (specifically leaf) accumulation.

The effect of plant size on the numerical values of scaling exponents was insignificant above the threshold of 1-year-old plants. When the data in the large size ranges were sorted into

Table 1. Statistical comparisons among standing M_L, M_S, and M_R relations across seed plants and within angiosperm and conifer data sets. Scaling exponents and allometric constants are for reduced major axis regression ($\alpha_{RMA} \pm$ SE and $\beta_{RMA} \pm$ SE) of $\log_{10}$-transformed data (original units in kg of dry weight per plant). In all cases, $P < 0.0001$.

	$\alpha_{RMA} \pm$ SE			$\beta_{RMA} \pm$ SE			
Y_1 versus Y_2	Predicted	Observed	95% CI	Observed	r^2	n	F
Across all data sets							
M_L versus M_S	0.75	0.75 ± 0.008	0.73–0.76	0.12 ± 0.012	0.910	661	8,425
M_L versus M_R	0.75	0.79 ± 0.016	0.76–0.82	0.41 ± 0.016	0.861	338	2,439
M_S versus M_R	1.00	1.09 ± 0.009	1.05–1.13	2.59 ± 0.012	0.971	366	13,621
Angiosperm interspecific data sets							
M_L versus M_S	0.75	0.73 ± 0.008	0.71–0.74	0.13 ± 0.075	0.924	622	7,537
M_L versus M_R	0.75	0.76 ± 0.015	0.74–0.79	0.30 ± 0.019	0.920	217	2,466
M_S versus M_R	1.00	1.10 ± 0.012	1.08–1.12	2.61 ± 0.017	0.977	221	9,129
Conifer interspecific data sets							
M_L versus M_S	0.75	0.78 ± 0.015	0.74–0.81	0.34 ± 0.074	0.863	350	2,198
M_L versus M_R	0.75	0.86 ± 0.029	0.79–0.92	0.76 ± 0.035	0.802	172	689
M_S versus M_R	1.00	1.10 ± 0.019	1.06–1.14	2.73 ± 0.022	0.951	171	3,282
Mean exponent of intraspecific datasets							
M_R versus M_A	~1.00	0.98 ± 0.11	0.885–1.09	–	–	–	32

[1]Department of Ecology and Evolutionary Biology, University of Arizona, Tucson, AZ 87519, USA. [2]Center for Applied Biodiversity Science, Conservation International, 1919 M Street N.W., Suite 600, Washington, DC 20036, USA. [3]Department of Plant Biology, Cornell University, Ithaca, NY 14853, USA.

*To whom correspondence should be addressed. E-mail: benquist@u.arizona.edu

different size ranges, separate regression analyses failed to detect statistically significant differences in the scaling exponents for M_L, M_S, and M_R relations. For example, regression of M_L versus $+3 < \log_{10} M_R < -0.5$ obtained a scaling exponent of 0.77 ± 0.02 (95% CI = 0.74 to 0.81, $r^2 = 0.783$, $n = 337$, $F = 1208$, $P < 0.0001$), whereas regression of M_L versus $-0.5 \leq \log_{10} M_R < +3$ obtained a scaling exponent of 0.79 ± 0.04 (95% CI = 0.68 to 0.89, $r^2 = 0.539$, $n = 183$, $F = 211.3$, $P < 0.0001$). Slight deviations were observed for allocation exponents involving M_R (Table 1). This is likely due to increased error in sampling the smallest roots from large trees.

Compilations of intraspecific variation in M_A and M_R during ontogeny provide strong additional support for our theory. Across 61 species of woody tree and large shrub species, the average scaling exponent for M_L versus basal stem diameter scales is 2.17 (95% CI = 2.01 to 2.32, mode = 2.06, $n = 61$). This numerical value is essentially indistinguishable from that predicted or observed within or across our data sets. Furthermore, as predicted, the average intraspecific exponent for the scaling of root and shoot biomass (M_A) during ontogeny across 32 independent studies including 26 species of herbaceous and woody plant species is 0.98 (95% CI = $1.09 \leq \alpha_{RMA} \leq 0.885$). These exponents also agree with data reported for a limited number of studies treating individual species or individual community samples of comparable geographic scale (*2*), although it is evident from our theory that a maternal compartment can influence shoot-to-root ratios for especially small, juvenile plants.

The scaling exponents predicted by the model also appear to be insensitive to ecological factors known to influence local community composition, abundance, and average plant size. For example, whereas average M_T per community is inversely proportional to the number of plants per ha, $M_T \propto N^{-4/3}$ or $N \propto M_T^{-3/4}$ in accordance with allometric theory (*12*), the scaling exponents for biomass allocation do not vary across diverse communities differing by over five orders of magnitude in average plant size (Fig. 3). Despite the residual variation in organ and M_T attributable to plants grown under stressful conditions [e.g., drought, light deprivation, or elevated ultraviolet-B (UV-B levels)], statistical outliers are once again comparatively rare.

The ability to predict the absolute amounts of M_L, M_S, or M_R at the level of both the individual plant or an entire community is limited, because significant variation exists in the numerical values of allometric "constants" across species. For example, although both angiosperm and gymnosperm M_L scales as the 3/4 power of M_S (Table 1), the corresponding allometric constants (β_{RMA} values = the y intercepts) significantly differ from each other (i.e., 0.13 ± 0.075 and 0.34 ± 0.074, respectively)

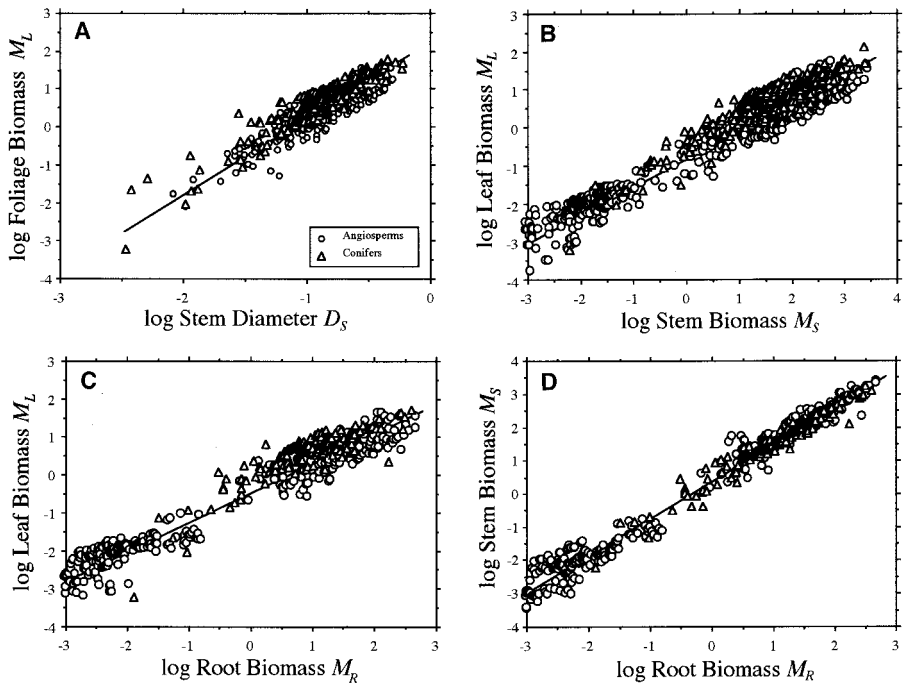

Fig. 1. D_S and M_L, M_S, and M_R relations for average plants from worldwide data sets. Solid lines are reduced major axis regression curves of log-transformed data. Angiosperm and conifer species are denoted by circles and triangles, respectively. (**A**) M_L versus D_S (trunk diameter at breast height). (**B**) M_L versus M_S. (**C**) M_L versus M_R ($r^2 = 0.861$, $n = 338$, $F = 2439$, $P < 0.0001$). (**D**) M_S versus M_R. See Table 1 for additional statistics. Note, the relatively larger spread in (B) and (C) is due to differences between Angiosperms and Gymnosperms.

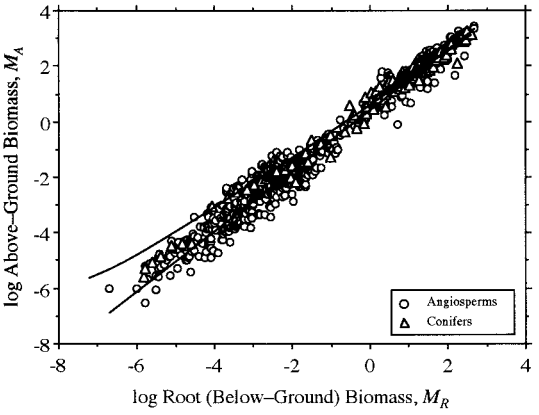

Fig. 2. M_A versus M_R. Angiosperm and conifer species are denoted by circles and triangles, respectively. Log-log nonlinear curve denotes predicted values of M_A based on theory [i.e., $M_S + M_L = (\beta_{12}/\beta_{13})M_R + (M_R/\beta_{13})^{3/4}$] (*16*), with empirical values of M_R with $\beta_{12} = 8.33$ and $\beta_{13} = 2.44$; the log-log linear curve denotes the best statistical fit of actual data.

(Table 1). Thus, for equivalent M_S, conifers have, on average, 2.6 times more M_L than do angiosperms. This observation resonates with the fact that conifers typically retain three cohorts of leaves that have less well-developed aerenchymatous mesophyll as compared with angiosperm leaves. Yet, even though conifer wood tends to be less dense than angiosperm wood, angiosperms and gymnosperms do not differ in the allometric relation between total M_R and M_A nor with the scaling of plant density and M_A (Figs. 2 and 3).

Plant biologists have long held the opinion that much idiosyncratic and site-specific variation exists in biomass allocation both within and across plant taxa, especially during ontogeny (*23*). Taxon and site-specific variation in biomass allocation is well known in response to differential selection for adaptations to different environmental conditions (e.g., species adapted to arid and hot conditions tend to have reduced M_L with respect to M_S or M_R) (*23*, *24*). Nevertheless, when viewed across a large range of plant sizes, the about 10-fold variation in biomass allocation shown in Figs. 1 through 3 is slight as compared with the striking invariance observed (and predicted) for the scaling exponents of M_L, M_S, and M_R across an impressive ~nine orders of magnitude of M_T across diverse communities differing in latitude and elevation. Traditionally, this variation has been indexed by ratios (e.g., stem:leaf, root:shoot, etc.). How-

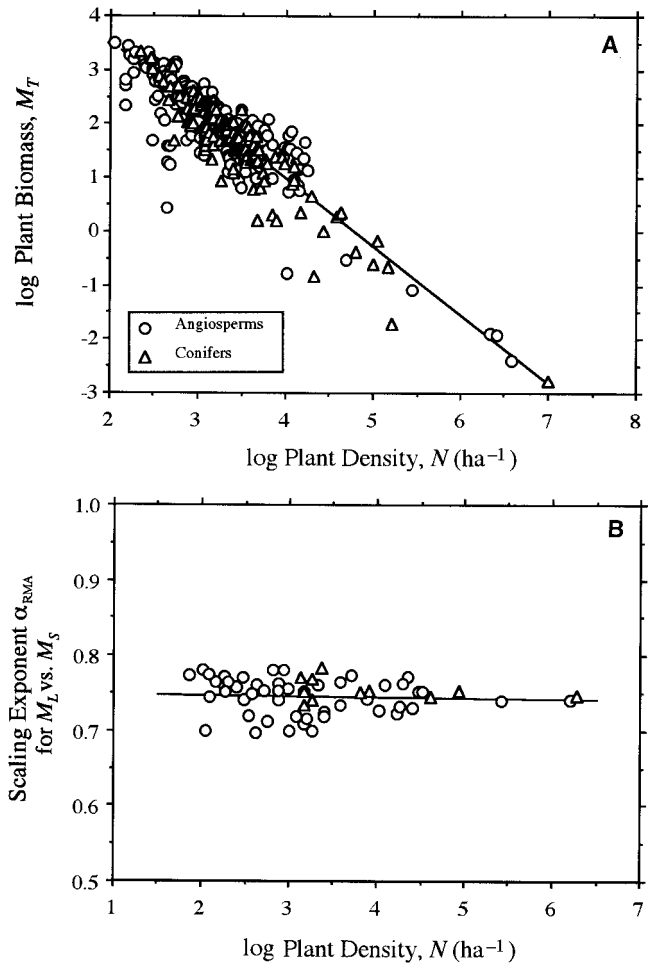

Fig. 3. Effects of plant density (number of plants per ha, N) on individual plant M_T and the scaling exponent (slope of reduced major axis regression curve, α_{RMA}) for the relation between individual plant M_L and M_S. Data were taken from Cannell data sets (*19*, *20*). Angiosperm and conifer species are denoted by circles and triangles, respectively. (**A**) M_T is inversely proportional to N, $M_T \propto N^{-1.33}$ (95% CI = $-1.41 \leq \alpha_{RMA} \leq -1.26$; $r^2 = 0.787$, $n = 298$, $F = 1096$, $P < 0.0001$). (**B**) Numerical value of scaling exponent for the relation between M_L and M_S (Fig. 1B) does not vary significantly as a function of N ($r^2 = 0.0002$, $n = 64$, $F = 0.017$, $P = 0.817$).

ever, ratios fail to capture the actual functional relations characterizing biomass allocation among organ types. In contrast, our model and empirical findings quantitatively define the numerical limits on plant allocation strategies, which incidentally accord well with the observation that M_A and M_R are not significantly correlated with site age, absolute latitude, elevation, or number of species within the community. Furthermore, expressing allocation in terms of functional allometric relation provides a baseline by which to assess residual variation. For example, residual variation in biomass allocation between roots and shoots is significantly, although very weakly, correlated with plant height ($P < 0.0001$, $r^2 = 0.058$, $n = 271$) and local productivity ($P = 0.007$, $r^2 = 0.04$, $n = 178$).

Our model provides strong bridges to more detailed biometric analyses of individual plants within and across communities (*10*, *25*). Furthermore, in conjunction with the allometric relation predicted by a growing body of allometric theory (*12–15*, *26*), a general allometric framework directly pertains to developing quantitative models for global climate as well as a variety of other important ecological and evolutionary phenomena including the approximate boundary conditions for difficult-to-measure M_R (*1–10*). Also, by identifying fundamental biomass partitioning rules, the model helps to identify the biophysical constraints acting on allocation tradeoffs in plant biology that potentially extend into the fossil record when seed plants first evolved. Allometric theory therefore holds great promise as a powerful quantitative tool with which to predict past and present-day plant structure-function relation at the level of the individual, community, or entire ecosystem (*26*).

References and Notes

1. J. P. Caspersen *et al*., *Science* **290**, 1148 (2000).
2. F. A. Bazzaz, J. Grace, *Plant Resource Allocation* (Academic Press, New York, 1997).
3. R. P. Detwiler, C. A. S. Hall, *Science* **239**, 42 (1988).
4. S. Levis, J. A. Foley, D. Pollar, *J. Clim.* **13**, 1313 (2000).
5. D. Tilman, C. L. Lehman, K. T. Thomson, *Proc. Natl. Acad. Sci. U.S.A.* **94**, 1857 (1997).
6. I. F. Wardlaw, *New Phytol.* **116**, 341 (1990).
7. K. J. Niklas, *Plant Allometry* (Univ. of Chicago Press, Chicago, 1994).
8. Y. Iwasa, J. Roughgarden, *J. Theor. Biol.* **25,** 78 (1984).
9. E. L. Charnov, *Nature* **387**, 393 (1997).
10. S. Brown, *Food Agric. Org. United Nations For. Pap.* (Food and Agriculture Organization of the United Nations, Rome, Italy) **134**, 5 (1997).
11. M. G. R. Cannell, R. C. Dewar, *Adv. Ecol. Res.* **25**, 59 (1994).
12. B. J. Enquist, J. H. Brown, G. B. West, *Nature* **395**, 163 (1998).
13. B. J. Enquist, G. B. West, E. L. Charnov, J. H. Brown, *Nature* **401**, 907 (1999).
14. G. B. West, J. H. Brown, B. J. Enquist, *Nature* **400**, 655 (1999).
15. K. J. Niklas, B. J. Enquist, *Proc. Nat. Acad. Sci. U.S.A.* **98**, 2928 (2001).
16. Noting that $B = \beta_1$, $M_T^{3/4} = \beta_1(M_L + M_S + M_R)^{3/4}$, and $B = \beta_2 M_L$, where β_1 and β_2 include units of years^{-1}, we obtain $M_L = \beta_3(M_L + M_S + M_R)^{3/4}$, where $\beta_3 = \beta_1/\beta_2$. Because, for any species, $M_S = \beta_4\rho_S D_S^2 L_S$ and $M_R = \beta_5\rho_R D_R^2 L_R$, where ρ is stem or root tissue bulk density, L is organ length, and D_R is root diameter, and because $\beta_4\rho_S$ and $\beta_5\rho_R$ are constant (i.e., denoted by β_6 and β_7, respectively), we also see that $M_L = \beta_3(M_L + \beta_6 D_S^2 L_S + \beta_7 D_R^2 L_R)^{3/4}$. This relation can be solved for M_L by imposing a minimum "cost" constraint so that that the total volume of water absorbed and transported by roots through stems per unit time is conserved such that D_R^2 is proportional to D_S^2 (*17*, *18*, *27*). Thus, $M_L \propto \beta_8 D_S^2$ and $M_L \propto \beta_9 D_R^2$, where β_8 and β_9 are additional allometric constants reflecting the proportional allocation to root and shoot biomass. These scaling relations give $M_L = \beta_3[1 + (\beta_6/\beta_8)\ L_S + (\beta_7/\beta_9)L_R]^{3/4}(M_L)^{3/4}$ and thus $M_L = \beta_3^4[1 + (\beta_6/\beta_8)L_S + (\beta_7/\beta_9)L_R]^3$. Allometric theory predicts that many biological lengths (such as root and shoot length) scale as $M^{1/4}$ ($L_S \propto M^{1/4}$ and $L_R \propto M^{1/4}$) (*12–15*). Therefore, it is expected that L_R and L_S scale isometrically to each other (i.e., $L_R = \beta_{10}L_S$). It therefore follows that $M_L = \beta_3^4[(1/L_S) + (\beta_6/\beta_8) + (\beta_7\beta_{10}/\beta_9)]^3 L_S^3$. Furthermore, because $1/L_S \rightarrow 0$ with increasing growth in size, we find that $M_L \sim \beta_3^4[(\beta_6/\beta_8) + (\beta_7\beta_{10}/\beta_9)]^3 L_S^3 = \beta_{11}L_S^3$. Therefore, our model predicts that $M_S = (\beta_6/\beta_8\beta_{11}^{1/3})$, $M_L M_L^{1/3} = \beta_{12}M_L^{4/3}$, $M_R = (\beta_7\beta_{10}/\beta_9\beta_{11}^{1/3})$, $M_L M_L^{1/3} = \beta_{13}M_L^{4/3}$, and $M_S = (\beta_{12}/\beta_{13})M_R$. The reciprocal of L_S appears in our derivations ($1/L_S$). This term approaches zero with increasing plant size but will affect the values of scaling exponents with M_S for very small plants. Thus, deviations in the predicted values of exponents are expected for plants smaller than those measured in this study. It also follows that the total M_A is a complex allometry equaling the sum of both the shoot and leaf biomass, $M_A = M_S + M_L = (\beta_{12}/\beta_{13})M_R + (M_R/\beta_{13})^{3/4}$. Thus, once an individual plant becomes photosynthetically self-sufficient and exhausts its maternal compartment contributing to early seedling development (i.e., angiosperm endosperm or conifer megagametophyte nutrients), M_A is predicted to scale nearly isometrically with respect to M_R.
17. C. D. Murray, *Proc. Nat. Acad. Sci. U.S.A.* **12**, 207 (1926).
18. C. R. Taylor, E. R. Weibel, *Resp. Physiol.* **44**, 1 (1981).
19. M. G. R. Cannell, *World Forest Biomass and Primary Production Data* (Academic Press, New York, 1982).
20. Data for specimens of mature tree species were collected from Cannell's (*19*) standardized tabulations, which include the complete primary citation and when-published longitude, elevation, the age of the dominant species (or conspecific) at each locality, the number of plants per 1.0 ha (plant density), height, total basal stem cross-sectional area, and standing biomass (in units of metric tons of dry matter per 1.0 ha) of stem wood, bark, branches, foliage, and roots. Values for standing organ biomass reflect as possible annual losses of dry matter due to mortality, litter-fall, decay, or consumption. In most cases, reported biomass values are based on direct measurements of fully dissected representative plants (typically ≥5 individuals) used in regression analyses to estimate M_T for each organ type per 1.0 ha. Most of the data are from even-age monospecific and mature stands (>25 years, $n = 600$ out of 880 complete data sets); the variance in reported values is thus comparatively small. Most studies undoubtedly underestimate M_R because of difficulty in extracting fine and small roots. Nevertheless, the vast majority of M_R is in the largest root branches, which are straightforward to sample. Additional data, especially for small monocot and dicot herbaceous species and juvenile (<1 year old) woody species, were gathered by K.J.N. from primary literature published between 1991 and 2001 (*22*). These data were from plants grown under a variety of natural field and experimental conditions (e.g., elevated UV-B or CO_2 levels and drought). Only two criteria were used to select data:

Data (i) had to have small variance (as gauged by reported SE) and (ii) had to be reported in units of kg of dry weight per plant. A total of 385 species are represented in the complete data set (including arborescent monocots, dicots, and conifers). Data for the intraspecific scaling of plant organ biomass were collected by B.J.E. primarily from the agricultural and forestry literature (*25*, *27*, *28*).

21. M_L, M_S, and M_R were each computed for an average plant from each community or experimental manipulation with the quotient of total plant biomass per site or treatment and plant density. Model type II (reduced major axis) regression analyses were then used to determine scaling exponents and allometric constants (regression slopes and *y* intercepts designated as α_{RMA} and β_{RMA}, respectively), because functional rather than predictive relation were sought among variables that were biologically interdependent and subject to unknown measurement error (*7*). Because many authors failed to report all of the necessary parameters required to assess M_L, M_S, and M_R, the sample size of regression analyses varies across statistical comparisons.
22. Supplementary materials can be found on *Science* Online at www.sciencemag.org/cgi/content/full/295/5559/1517/DC1.
23. F. A. Bazzaz, in *Plant Resource Allocation*, F. A. Bazzaz, J. Grace, Eds. (Academic Press, New York, 1997), pp. 1–37.
24. R. M. Callaway, E. H. DeLucia, W. H. Schlesinger, *Ecology* **75**, 147 (1994).
25. W. B. Smith, *Allometric biomass equations for 98 species of herbs, shrubs, and small trees* (North Central Forest Experimental Station Research Note NC-299, Forest Service U.S. Department of Agriculture, Washington, DC, 1983).
26. B. J. Enquist, K. J. Niklas, *Nature* **410**, 655 (2001).
27. W. H. Pearsall, *Ann. Bot.* **41**, 549 (1927).
28. C. Monk, *Bull. Torrey Bot. Club* **93**, 402.20 (1966).

29. We thank E. Charnov, A. Ellison, D. Ackerly, H.-C. Spatz, L. Sack, and D. Raup for discussions or comments on earlier drafts of this manuscript. This work stems as an outgrowth of discussions from the Body Size in Ecology and Evolution Working Group (F. A. Smith, principle investigator) sponsored by The National Center for Ecological Analysis and Synthesis. B.J.E. was supported by NSF; K.J.N. was supported by an Alexander von Humboldt Forschungspreis and New York State Hatch grant funds.

19 September 2001; accepted 7 December 2001

Enzyme Dynamics During Catalysis

Elan Zohar Eisenmesser,[1] Daryl A. Bosco,[1] Mikael Akke,[2] Dorothee Kern[1]*

Internal protein dynamics are intimately connected to enzymatic catalysis. However, enzyme motions linked to substrate turnover remain largely unknown. We have studied dynamics of an enzyme during catalysis at atomic resolution using nuclear magnetic resonance relaxation methods. During catalytic action of the enzyme cyclophilin A, we detect conformational fluctuations of the active site that occur on a time scale of hundreds of microseconds. The rates of conformational dynamics of the enzyme strongly correlate with the microscopic rates of substrate turnover. The present results, together with available structural data, allow a prediction of the reaction trajectory.

Although classical enzymology together with structural biology have provided profound insights into the chemical mechanisms of many enzymes (*1*), enzyme dynamics and their relation to catalytic function remain poorly characterized. Because many enzymatic reactions occur on time scales of micro- to milliseconds, it is anticipated that the conformational dynamics of the enzyme on these time scales might be linked to its catalytic action (*2*). Classically, enzyme reactions are studied by detecting substrate turnover. Here, we examine enzyme catalysis in a nonclassical way by characterizing motions in the enzyme during substrate turnover. Dynamics of enzymes during catalysis have previously been detected with methods such as fluorescent resonance energy transfer, atomic force microscopy, and stopped-flow fluorescence, which report on global motions of the enzyme or dynamics of particular molecular sites. In contrast, nuclear magnetic resonance (NMR) spectroscopy enables investigations of motions at many atomic sites simultaneously (*3*, *4*). Previous NMR studies reporting on the time scales, amplitudes, and energetics of motions in proteins, have provided information on the relation between protein mobility and function (*5*–*15*). Here, we have used NMR relaxation experiments to advance these efforts by characterizing conformational exchange in an enzyme, human cyclophilin A (CypA), during catalysis.

CypA is a member of the highly conserved family of cyclophilins that are found in high concentrations in many tissues. Cyclophilins are peptidyl-prolyl cis/trans isomerases that catalyze the interconversion between cis and trans conformations of X-Pro peptide bonds, where "X" denotes any amino acid. CypA operates in numerous biological processes (*16*, *17*). It is the receptor for the immunosuppressive drug cyclosporin A, is essential for HIV infectivity, and accelerates protein folding in vitro by catalyzing the rate-limiting cis/trans isomerization of prolyl peptide bonds (*18*, *19*). However, its function in vivo and its molecular mechanism are still in dispute. X-ray structures of CypA in complex with different peptide ligands show cis X-Pro bonds (*20*, *21*), except for a trans conformation in the CypA/HIV-1 capsid complex (*22*, *23*). In each case, only one conformer was observed in the crystal, even though both isomers must bind to CypA for catalysis of cis/trans isomerization to occur.

We characterized motions in CypA during catalysis with the use of ^{15}N spin relaxation experiments with and without the substrate Suc-Ala-Phe-Pro-Phe-4-NA (*24*). Longitudinal (R_1) and transverse (R_2) auto-relaxation rates, transverse cross-correlated cross-relaxation rates (η_{xy}), and $\{^1H\}$-^{15}N nuclear Overhauser enhancements (NOE) were measured for all backbone amides in CypA (*25*). Though all parameters are sensitive to "fast" motions (pico- to nanoseconds), only R_2 is sensitive to "slow" conformational exchange (micro- to milliseconds) (*5*–*8*). A progressive substrate-induced shift for several CypA amide resonances (Fig. 1) indicates catalysis-linked motions. It shows (i) that these amides experience different magnetic environments in free CypA (E) and in CypA bound to substrate (ES) and (ii) that the

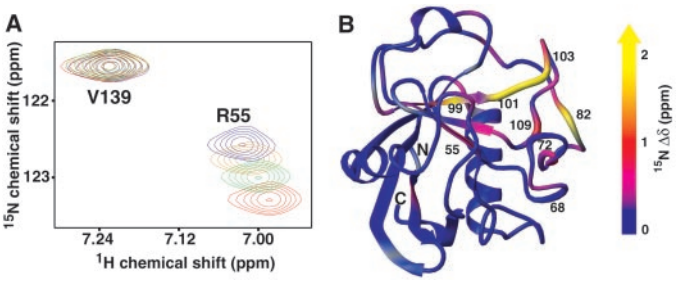

Fig. 1. Chemical shift changes of the amide signals in CypA upon titration with the substrate Suc-Ala-Phe-Pro-Phe-4-NA. (**A**) At a constant CypA concentration of 0.43 mM, spectra were recorded at 0 mM (blue), 0.38 mM (orange), 1.01 mM (green), and 2.86 mM (red) substrate. The signal of R55 is progressively shifting upon addition of increasing amounts of substrate, indicating fast conformational exchange during catalysis. The observed chemical shifts are population-weighted averages of E and ES, and thus shift towards the position of the ES complex with increasing amounts of substrate. In contrast, the signal of V139 is not affected by catalysis. (**B**) The chemical shift differences between free CypA and in the presence of 2.86 mM substrate were mapped onto the structure (1RMH) (*21*) with the use of a continuous color scale.

[1]Department of Biochemistry, Brandeis University, Waltham, MA 02454, USA. [2]Department of Biophysical Chemistry, Lund University, Post Office Box 124, SE-221 00 Lund, Sweden.

*To whom correspondence should be addressed. E-mail: dkern@brandeis.edu